Theoretical Study of the Adsorption of Acetylene on the (111) Surfaces of Pd, Pt, Ni, and Rh

J. Will Medlin† and Mark D. Allendorf*

Combustion Research Facility, Sandia National Laboratories, Livermore, California 94551

Received: July 17, 2002; In Final Form: November 8, 2002

Plane-wave density functional theory and extended Hückel calculations have been used to study the adsorption of acetylene and hydrogen on the (111) surface planes of Pd, Pt, Ni, and Rh. In agreement with previous experimental and computational studies, atomic hydrogen is found to preferentially adsorb in a 3-fold hollow site on each metal surface, although the potential-energy surface for hydrogen binding is apparently rather flat. Differences in the adsorption behavior of acetylene on the four surfaces are more pronounced. An adsorption structure in which C_2H_2 is oriented above a 3-fold hollow, with its axis parallel to but tilted away from a metal−metal bond, is computed to be most stable on Pd, Pt, and Rh. On Ni(111), acetylene is found to strongly adsorb above two contiguous hollow sites, with its molecular plane perpendicular to the surface and bisecting a Ni−Ni bond. The anomalous adsorption behavior on Ni is explained using the crystal orbital Hamilton population formalism. Calculated C_2H_2 adsorption behavior is compared with experimental studies of acetylene decomposition and hydrogenation on single-crystal surfaces. Implications for the mechanism of acetylene hydrogenation on supported metal catalysts are also discussed.

1. Introduction

The industrial manufacture of high-purity ethylene often requires the removal of small amounts of acetylene from the post-cracking feed. This can be accomplished via the autothermal hydrogenation of acetylene to ethylene over supported metal catalysts.[1] Because ethylene is the desired reaction product, the key parameter in discriminating between different catalyst formulations is selectivity to ethylene, as opposed to the full hydrogenation product ethane. Numerous metals are effective for the partial hydrogenation of acetylene, but supported Pd catalysts have been shown to exhibit especially high ethylene selectivities.[2] Interestingly, experimental studies of acetylene hydrogenation catalysts have shown that a carbonaceous layer accumulates on the metal surface after bringing the catalyst on-stream.[3,4] This carbonaceous material reduces the catalytic activity and remains present on the surface under steady-state reaction conditions. The mechanism for acetylene hydrogenation has been the subject of considerable debate, with various suggestions concerning the reactive state of acetylene, the high selectivity shown by certain catalysts, and the role of the carbonaceous layer.[5−9]

Insights into the possible reaction pathways of acetylene and hydrogen on various metals have been provided by controlled studies on single-crystal surfaces. Acetylene has been shown to interact strongly with late transition-metal surfaces. On the (111) surface planes of Pd,[10] Pt,[11] Ni,[12] and Rh,[13] chemisorbed acetylene decomposes at low temperature to produce a number of surface intermediates, including vinylidene ($-CCH_2$), acetylide ($-CCH$), ethylidyne ($-CCH_3$), methylidyne ($-CH$), and surface carbon. When the surface is also partially covered with atomic hydrogen, these surface species can undergo hydrogenation. For example, on Pd(111), adsorbed acetylene can be converted to ethylene and vinylidene can be hydrogenated to ethylidyne.[14−16] A large body of experimental evidence shows that the acetylene reactivity varies significantly on the Pd, Pt, Ni, and Rh surfaces, with the reaction energetics and prevalence of various surface species differing depending on the surface metal. Identification of reasons for differences in acetylene reactivity requires a better understanding of the interaction of the acetylene molecule with these surfaces. Elucidating the nature of the acetylene−surface interaction for these metals may also shed light on the mechanism of important catalytic reactions, such as acetylene hydrogenation.

Computational chemistry studies can be very useful in understanding the interaction of adsorbates with single-crystal metal surfaces. An advantage of these studies is that they allow for the straightforward determination of binding energies for a range of different adsorption structures, information that is difficult to measure experimentally.[17] This binding energy information can be used to develop a better understanding of reactant−catalyst interactions, which in turn can help explain trends in catalytic behavior. Computational investigations of acetylene adsorption using varying degrees of complexity have previously been conducted on Pt,[18] Pd,[19] and Ni[20] (111) surfaces. Although these studies provide important insight into the preferred acetylene binding site for each metal, it is difficult to make direct comparisons between different sets of calculations performed for different metal surfaces. To address how differences in acetylene binding on metals may affect subsequent reactivity, we have performed a self-consistent series of plane-wave density functional theory (DFT) calculations to assess the adsorption behavior of hydrogen and acetylene on the (111) surface planes of Pd, Pt, Ni, and Rh. These metal surfaces were selected because of the broad general interest in catalysis by these four metals. Hydrogen adsorption has been well studied on these surfaces;[21−23] we include only a brief description of these calculations here to serve as a benchmark for other

* To whom correspondence should be addressed. E-mail: mdallen@sandia.gov.

† Present address: Department of Chemical Engineering, University of Colorado, Boulder, CO 80309.

10.1021/jp026555t CCC: $25.00
Published on Web 12/10/2002

calculations and to verify that direct comparisons between metals can be accurately made. Our discussion is heavily focused, however, on comparisons of acetylene adsorption behavior on different metal surfaces. The computed acetylene adsorption behavior is also compared with previous experimental and computational studies of acetylene adsorption on the (111) surface planes of Pd, Pt, Rh, and Ni. Finally, implications of this work for the mechanism of acetylene hydrogenation on supported catalysts are discussed.

2. Computational Details

The CASTEP software program[24] was used to perform all plane-wave DFT calculations, utilizing the GGA-PW91[25] level of theory with Vanderbilt ultrasoft pseudopotentials.[26] Computations were performed over a range of *k*-point spacings (as generated by the Monkorst−Pack scheme[27]) and kinetic energy cutoff values to ensure that convergence of the computed total energy was achieved. In general, the results reported here are for *k*-point spacings of <0.05 Å^{-1} with the following metal-dependent cutoff energies: 280 eV for Pt, 340 eV for Pd and Ni, and 310 eV for Rh.

Geometry optimizations were performed on supercell structures using periodic boundary conditions. The (111) surfaces were generally modeled using metal slabs with a thickness of 3 atomic layers, although selected calculations were performed on 6-layer slabs. The surface unit cell size was specified to generate the desired adsorbate coverage. The vacuum spacing between slabs was held at 10 Å for all computations. Although symmetry was imposed during initial calculations in order to identify reasonable adsorption structures, all results reported here correspond to fully relaxed slabs, with no symmetry constraints placed on the metal−adsorbate system.

The adsorption energies for hydrogen and acetylene on (111) metal surfaces have been computed using the following equations:

$$\text{For H:}\quad \Delta H_{ads} \approx E_{ads} = E_{M-H} - E_M - \frac{1}{2}E_{H_2} \qquad (1)$$

$$\text{For } C_2H_2\text{:}\quad \Delta H_{ads} \approx E_{ads} = E_{M-C_2H_2} - E_M - E_{C_2H_2} \qquad (2)$$

where the first term on the right-hand side of each equality is the total energy of the adsorbate-covered slab, the second term is the energy of the bare metal slab, and the final term corresponds to the energy of the gas phase "reactant" molecule. Computed adsorption energies are at 0 K and do not account for zero-point energy effects. Note that the adsorption energy of hydrogen defined by eq 1 should theoretically be equal to $^1/_2$ of the adsorption energy of hydrogen measured in a typical experiment. Experimental adsorption energy values for hydrogen quoted in the text below have already been multiplied by the $^1/_2$ factor for the purposes of direct comparison.

Extended Hückel calculations were performed using "Yet Another extended Hückel Molecular Orbital Package" (YAeHMOP), a program freely available on the Web.[28] Although less suitable for total energy calculations than DFT methods, extended Hückel calculations allow one to analyze chemical bonds to surfaces in a much more straightforward manner.[29−31] This analysis is accomplished here using the crystal overlap Hamilton population (COHP) formalism, [32,33] which allows one to compute the energetic bonding and antibonding contributions of orbital overlaps between molecules. DFT-optimized geometries were used for the YAeHMOP COHP calculations, and *k*-point spacings were also set to those used in DFT. Default extended Hückel parameters were employed for all elements in the calculation.

TABLE 1: Site Adsorption Energies (in kcal/mol) for Atomic H on (111) Metal Surfaces at 1/4 ML Coverage[a]

	Pd	Pt	Rh	Ni
atop	−4.0	−14.5	−5.0	−7.8
bridge	−11.3	−15.0	−13.3	−13.3[b]
hcp	−14.3	−13.5	−16.4	−14.7
fcc	−15.0	−16.1	−16.7	−13.8

[a] Calculations were on 3-layer metal slabs with symmetry constraints fully relaxed. [b] Bridge geometry was not stable on Ni with full relaxation of symmetry constraints; the reported value is for an H atom constrained in the bridge position.

3. Results and Discussion

3.1. Adsorption of Hydrogen. The adsorption of hydrogen on the (111) surfaces of Rh, Pd, Ni, and Pt has been studied extensively and is treated only briefly here to provide a benchmark for comparison with the less well-understood acetylene system. Four symmetric sites for H adsorption were considered, with H atoms alternately located in the atop, bridge, and both the hcp and fcc 3-fold-hollow positions above the metal surface. (The hcp and fcc hollow sites are defined as being located directly above a second- and third-layer metal atom, respectively.) Full geometry optimizations were performed for each of these configurations at both 1 monolayer (ML) and 0.25 ML coverages using a metal slab thickness of 3−6 atomic layers. Decreasing coverage was found to have only a small (1−4 kcal/mol) stabilizing effect on hydrogen adsorption energies; therefore, only the $^1/_4$ ML results are discussed below. Table 1 lists computed H binding energies for all four metals and indicates that trends in the hydrogen adsorption energy at different binding sites are quite similar for Pd, Ni, and Rh surfaces. For each of these metals, adsorption in the hollow positions is preferred, as predicted by previous experimental[34,35] and theoretical[21,36,37] studies. The relative uniformity of the binding energies at different metal sites suggests that the barrier for diffusion along this path is quite low and that H atoms may be expected to diffuse rapidly across the Rh, Ni, and Pd surfaces through "channels" around the atop positions.[37] For hydrogen adsorption on Pt (111), the atop position is found to be significantly stabilized, so that the atop, bridge, and hollow sites are all found to be nearly indistinguishable in terms of hydrogen adsorption energy. This is consistent with previous work by Papoian et al., who also found that the potential-energy surface is very flat for the H/Pt(111) system, and related this to the high level of Pt d-orbital (as opposed to s-orbital) participation in H binding to the surface.[22] The flatness of the potential-energy surface indicates that the barrier to surface diffusion of H, even across the atop position, should be quite low. The lack of adsorption site specificity may also allow the H-covered surface to accommodate any other adsorbate that preferentially covers specific Pt(111) sites. Although the atop position is less stable for H adsorbed on the (111) surfaces of Pd, Ni, and Rh, the uniformity of the potential-energy surface between the hollow and bridge positions implies a similar situation for these metals. Moreover, the high degree of similarity between the computed binding energies for the various sites on each metal suggests that any variations in acetylene hydrogenation reactivity among the metals are not attributable to differences in adsorption of hydrogen.

Table 2 shows the calculated adsorption energy and geometry for H atoms bound to the most stable site for each metal at $^1/_4$ ML coverage. The binding energy is shown for calculations

TABLE 2: Computed Hydrogen Adsorption Energies (Energies in kcal/mol) and Geometries (Distance in Å) for the Most Stable Structures on the (111) Surfaces of Pd, Pt, Ni, and Rh at 1/4 ML Coverage[a]

	Pd	Pt	Ni	Rh
preferred site	fcc	fcc	fcc	hcp
$-E_{ads}$	15.0	16.1	16.7	14.7
(3 layer slab)				
$-E_{ads}$	16.3	13.7	18.1	18.9
(6 layer slab)				
$-E_{ads}$	10[b]	8−12[c]	11[d]	9−10[e]
(experiment)				
H-surface plane distance	0.88	0.85	0.92	0.94
H−M atom distance	1.80	1.86	1.69	1.85

[a] Geometric parameters are given for the 6-layer slab calculation, although the parameters were nearly independent of slab size. [b] Reference 38. [c] References 39−41. [d] Reference 42. [e] References 43 and 44.

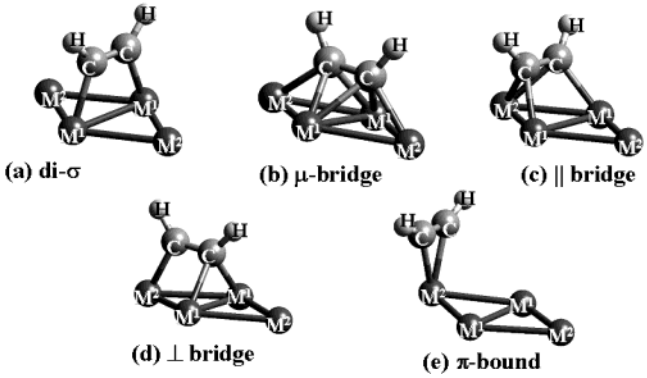

Figure 1. Schematic of adsorption structures for acetylene on (111) metal surfaces: (a) di-σ; (b) μ-bridge; (c) parallel-bridge (also denoted fcc-par or hcp-par); (d) perpendicular-bridge (fcc-perp and hcp-perp); (e) π (or atop). Adsorption positions are indicated relative to an M^1-M^1 bridge, with M^2 atoms completing each 3-fold hollow. Note that an hcp hollow site is located above a second-layer metal atom, and an fcc hollow site is located above a third-layer metal atom; the difference between these sites is not depicted in the figure. Chemical bonds are drawn to guide the eye but are not intended to describe the nature of bonding with the surface.

utilizing fully relaxed slabs of both 3-layer and 6-layer thicknesses. Slab thickness has little effect on the computed adsorption energy and no real effect on the optimized geometry; bond distances are only reported for the 6-layer slab calculations. Similarly, increases in the number of *k*-points and the energy cutoff yielded only small variations in computed binding energies. Table 2 also compares computed adsorption energies to those measured experimentally. Note that the calculated binding energies appear to be higher by roughly 5 kcal/mol; this error is most likely attributable to the neglect of zero-point energy (ZPE) and specific heat effects. In any case, the error appears to be approximately the same for each metal. Because the primary focus of this paper is on making comparisons among different adsorption sites and metals rather than on calculating absolute energy values, the small systematic error is acceptable for our purposes.

3.2. Adsorption of Acetylene. The adsorption of acetylene on (111) metal surfaces has been studied by both theoretical and experimental methods. At least seven possible symmetric adsorption structures have been identified for acetylene on the (111) plane; ball-and-stick representations of the structures are shown in Figure 1. The configurations denoted as parallel and perpendicular bridge structures may be located above either an fcc or hcp hollow site. In the remainder of the text, these sites are distinguished by the labels fcc-par and hcp-par for the parallel bridge and by the labels fcc-perp and hcp-perp for the perpendicular bridge. As in the studies of hydrogen, symmetry was imposed for initial calculations on each of the seven structures, but final geometry optimizations included the relaxation of all symmetry constraints. A consequence of this strategy is that not all adsorption geometries are found to be stable on each metal. Table 3 shows the binding energy computed at 1/4 ML coverage for each structure across the metal series Pd, Pt, Ni, and Rh, where missing cells in the table correspond to unstable structures. In addition, Table 4 provides a list of the adsorption energies and geometric parameters for the most stable adsorption structure on each metal. As in the case of hydrogen adsorption, Table 4 shows that the choice of a 3- versus 6-layer slab for the calculations has little effect on the computed adsorption energies. Because this system is far more complex than hydrogen adsorption, we will largely discuss the results for each metal sequentially. After considering binding trends on all four metals, we discuss possible reasons for differences in adsorption trends among the individual metals using COHP analysis of acetylene binding. We note here that for all metals considered, the π adsorption structure is the least stable because of its coordination to only a single metal atom on the surface. This is reflected in the geometry of the adsorbate, which is closer to that of the gas phase compared to the geometries calculated for other adsorption structures: the C−C bond length is increased only to ca. 1.25 Å (from a computed gas-phase value of 1.19 Å), and the C−C−H bond angle decreased to ca. 150° (from 180°). This represents a much less rehybridized structure than the more stable geometries described in Table 4. Reasons for stability trends for other sites across the metals are less transparent and thus are considered individually by metal below.

TABLE 3: Site Adsorption Energies (in kcal/mol) for Acetylene on (111) Metal Surfaces at 1/4 ML Coverage[a]

	Pd	Pt	Rh	Ni
μ-bridge	−47.3		−55.5	−68.2
p	−20.9	−16.9	−29.4	−32.9
hcp-perp	−47.8	−47.5	−55.2	
fcc-perp	−47.1	−49.8	−52.8	
hcp-par	−51.6	−49.6	−61.6	−62.1
fcc-par	−51.9	−54.7	−53.1	−61.6
di-σ	−43.0	−45.9		−45.1

[a] Calculations were on 3-layer metal slabs with symmetry constraints fully relaxed.

TABLE 4: Computed Acetylene Adsorption Energies (Energies in kcal/mol) and Geometries (Distance in Å) for the Most Stable Structures on the (111) Surfaces of Pd, Pt, Ni, and Rh at 1/4 ML Coverage[a]

	Pd	Pt	Ni	Rh
preferred site	fcc-par	fcc-par	μ-bridge	hcp-par
$-E_{ads}$	51.9	54.7	68.2	61.6
(3 layer slab)				
$-E_{ads}$	53.1	51.2	68.6	67.3
(6 layer slab)				
C-surface distance	1.44	1.47	1.37	1.47
$C-M^1$ distance	2.00	2.00	1.99	2.01
$C-M^2$ distance	2.16	2.20	1.92	2.16
C−C−H angle	128°	126°	122°	126°
tilt angle[b]	14°	22°	0°	16°

[a] Geometric parameters are given for the 6-layer slab calculation, although the parameters were nearly independent of slab size. The measure of the angle between the C_2H_2 plane and the surface normal is referred to as the "tilt" angle. [b] Angle of molecular plane of acetylene with respect to the surface normal.

3.2.1. Acetylene on Pd(111). We consider first the case of acetylene adsorption on Pd(111), Pd being the only metal for

which all seven adsorption structures were computed to be stable. With the exception of the much weaker π adsorption mode, all of the geometries also lie within a fairly narrow range in energy. The parallel-bridge structures are computed to be the most stable, with a heat of adsorption of −52 kcal/mol. The parallel-bridge geometry was also found to be the most stable from previous NEXAFS experimental studies [45] and Pd cluster calculations. [19] The perpendicular- and μ-bridge structures are computed to have somewhat lower binding energies at ca. −47 to −48 kcal/mol. This suggests a very flat potential-energy surface for diffusion of acetylene between perpendicular and μ-bridge positions, consistent with previous calculations. [19] For both parallel- and perpendicular-bridge configurations, there appears to be no difference between binding at hcp versus fcc sites; that is, the presence or absence of second-layer Pd atoms does not affect acetylene adsorption above the hollows. Finally, the di-σ structure is less stable than the parallel-bridge geometries by ca. 10 kcal/mol. This lower adsorption energy for di-σ bound acetylene is probably related to its lower degree of coordination to the surface; the di-σ geometry is the only structure besides π-bound acetylene that does not bind to at least three metal atoms.

The C_2H_2/Pd(111) system has been the subject of intensive experimental study because of the production of benzene through a cyclotrimerization reaction, which is unique among this series of metals. [10,46] Although the preferred adsorption geometry calculated here is consistent with experiment, it is less clear that the predicted adsorption energies are in equally good agreement. The adsorption energy computed for acetylene is very high and would appear to be indicative of a state that does not readily desorb intact from the Pd(111) surface. That is, it is likely that C−H bond cleavage for such a strongly adsorbed species would be thermally activated at a lower temperature than that required for desorption. Microcalorimetric studies on the Pd(100) surface have measured a much lower acetylene heat of adsorption of ∼27 kcal/mol at 300 K. [47] Assuming that acetylene adsorption is not highly structure sensitive, this suggests that acetylene may also exist in a more weakly bound state (presumably at high coverage) on the surface not identified by these calculations. Furthermore, temperature-programmed desorption (TPD) investigations of the C_2H_2/Pd(111) system show that small amounts of acetylene desorb at relatively low temperature at high coverages. [46] This desorption state, however, may again be from a "second layer" of adsorbed acetylene similar to that observed for ethylene. [48] Further reaction of acetylene on the surface produces vinylidene, with other surface species being isolated at higher temperatures. [16] These results suggest that acetylene may adsorb in multiple sites on the surface, with the strongly adsorbed parallel-bridge species preferentially undergoing decomposition, most likely through the vinylidene intermediate. This decomposition could lead to the creation of the carbonaceous layer observed in steady-state reactions on supported acetylene hydrogenation catalysts. Once formed, the carbonaceous layer may block Pd sites, potentially preventing incoming acetylene from adsorbing with 3-fold coordination to the surface. Instead, a more weakly adsorbed acetylene species (perhaps similar to the π-bound species) may be adsorbed to the surface and may in fact be the adsorbate responsible for formation of ethylene.[4] In other words, the most strongly adsorbed surface intermediate may not be the one responsible for desired product formation.[49]

3.2.2. Acetylene on Pt(111). Similar to the case of Pd(111), most of the adsorption structures computed for Pt(111) were found to lie within a fairly narrow range in energy. Again, the parallel-bridge adsorption geometry is found to be the most stable, followed by the perpendicular-bridge configuration. Table 3 indicates that there is a small preference for adsorption above fcc (as opposed to hcp) hollows for these sites. In addition, the μ-bridge structure is not found to be stable on Pt(111); calculations using the μ-bridge configuration as the initial structure converge to one of the perpendicular-bridge geometries. Nevertheless, the energy barrier to diffusion perpendicular to the bridge is still expected to be small based on the small energy gradients across the bridge computed during geometry optimization. As with Pd(111), the di-σ mode of adsorption is somewhat less preferred. Thus, despite some small differences between the adsorption properties computed for Pt(111) and Pd(111), the overall conclusion is that acetylene adsorption should be rather similar for these surfaces.

The computed heat of adsorption for acetylene in the parallel-bridge site is in good agreement with the ∼ −50 kcal/mol value determined by previous cluster calculations [18] and by microcalorimetry on supported Pt catalysts. [50] In contrast to results from investigations on Pd(111), experimental studies indicate that adsorption of acetylene on Pt(111) at temperatures as low as 125 K results directly in reaction to form vinylidene. [11,51] Vinylidene disproportionates by 200 K to form ethynyl and vinyl, which react at higher temperatures to form ethylidene, ethylidyne, and surface carbon. A small amount of self-hydrogenation to ethylene is also observed, but no larger hydrocarbon products (i.e., benzene) are formed during temperature programmed desorption.[52] Because adsorption of acetylene is computed to be quite similar for the two metals, it is most likely that differences in the energetics of subsequent reaction steps account for the differences in acetylene reactivity on the Pd and Pt surfaces. However, the possible existence of a more weakly adsorbed state of acetylene on Pd(111) could also have an impact on the prevalence of particular surface reactions.

3.2.3. Acetylene on Rh(111). The energies computed for the various acetylene adsorption structures on Rh(111) follow similar trends to those computed for the Pd and Pt surfaces. Our calculations do indicate, however, a clear preference for interaction with the Rh(111) hcp hollow site. Adsorption in the parallel-bridge configuration is again found to be most favorable, with $E_{ads} = -62$ kcal/mol. Binding in the perpendicular- and μ-bridge positions is slightly higher in energy, although once more there is a similarity in the computed binding energies across different sites. Acetylene binding on Rh(111) shows a slight variation from the other surfaces, in that calculations employing the di-σ configuration did not converge even when symmetry constraints were imposed, indicating that this is not a stable adsorption site for acetylene. Perhaps the most significant distinction in comparing the Rh surface to Pt and Pd is simply the 7−10 kcal/mol binding energy difference for the most stable structure. This suggests that the Rh(111) surface may be slightly more reactive toward acetylene, in accord with suggestions from previous experimental studies.[53]

In experimental temperature-programmed studies, acetylene decomposes on Rh(111) at low temperature primarily to produce vinylidene species, along with small amounts of ethylidyne and acetylide.[13,54] Vinylidene further decomposes above 400 K to produce acetylide and methylidyne species. Although the reaction temperatures vary to some degree, the reaction of acetylene on Rh(111) follows a similar path to that on Pt(111), consistent with our calculations which indicate that the potential-energy surfaces for acetylene on these metals are quite similar. Raman vibrational studies of acetylene adsorbed on Rh catalysts

suggest that this stable acetylene binds to the surface in a parallel-bridge configuration,[55] in agreement with the results reported here.

3.2.4. Acetylene on Ni(111). The computed adsorption behavior of acetylene on Ni(111) shows marked differences to the results on the other surfaces. As shown in Table 3, the μ-bridge site is calculated as clearly the most stable binding geometry, consistent with experiment.[56] The −68 kcal/mol adsorption energy, which is in good agreement with previous experimental studies[57] and in reasonable agreement with previous cluster calculations,[20] is substantially higher than that for Pd(111) or Pt(111). Geometry optimizations performed using a perpendicular-bridge configuration as the initial guess were found to converge to the μ-bridge structure. Adsorption of acetylene in the parallel-bridge positions is computed to be 6−7 kcal/mol weaker than the most stable adsorption structure, and the di-σ configuration is considerably less stable than the structures that interact with 3-fold hollows. Overall, the energies of the various possible adsorption structures are found to be less uniform on Ni(111) than on the other surfaces, with a clear preference for adsorption at the most stable site, the μ-bridging position.

The differences in the computed adsorption behavior for acetylene on Ni are reflected in experimentally observed reactivity patterns. Between 190 and 260 K, acetylene adsorbed on Ni(111) reacts to form methylidyne species. [12] That is, whereas the first step in acetylene reaction on the (111) surfaces of Pd, Pt, and Rh is C−H bond cleavage, decomposition of acetylene on Ni(111) is initiated by C−C bond cleavage. C−H bond scission on Ni occurs only upon further heating to 260−350 K and ultimately results in the formation of acetylide and surface carbon species.[12] This reversal in the order in which bonds are cleaved may be attributable to adsorption of acetylene in the μ-bridging, rather than parallel-bridging, position on Ni(111), as discussed below.

3.2.5. COHP Analysis. In an attempt to identify explanations for the apparently anomalous adsorption behavior of acetylene on Ni(111), extended Hückel calculations have been used to generate COHP curves for study of the details of surface−adsorbate binding. COHP curves describing the overlap of acetylene C atomic orbitals with surface Ni 3d and 3s orbitals are shown in Figure 2. These curves are shown for both the fcc parallel-bridge structure (the most stable for Pd and Pt surfaces) and the μ-bridge configuration (the most stable for Ni(111)). Integrations of the COHP curves are also shown to the right and indicate the cumulative strength of bonding as a function of energy. One of the dominant features in the COHP curve for the μ-bridge geometry is a substantial bonding overlap of the Ni^2 3s atomic orbital with a C−C π^* antibonding orbital at an energy ca. 8 eV below the Fermi level E_f. In the parallel-bridge geometry, there is also an overlap of C−C π^* orbitals with surface 3s orbitals, in this case, those associated with atoms in the Ni^1 position. For both adsorption structures, this back-bonding component strengthens the surface−adsorbate binding. However, the 3s/π^* overlap of acetylene adsorption is much smaller in the parallel-bridge configuration, resulting in a substantially smaller decrease in the integrated COHP energy at the Fermi level, as well as a lower acetylene binding energy.

We suggest that the preference for acetylene adsorption in the μ-bridging site on Ni(111) is related to the high degree of overlap between Ni 3s orbitals and C−C antibonding orbitals in that configuration. As has been pointed out for the adsorption of hydrogen, methyl, and ethyl on metal surfaces, s orbitals tend to make much larger contributions to the binding of adsorbates

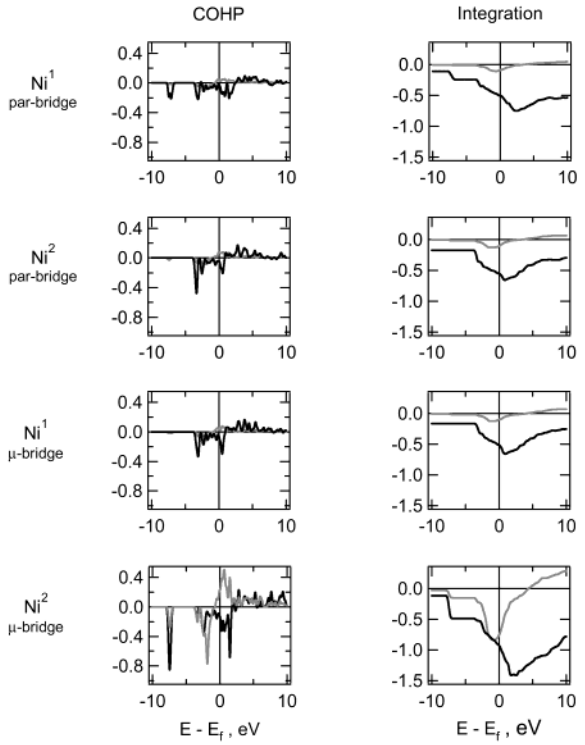

Figure 2. COHP curves (left column) and integrals (right column) for the overlap of C valence orbitals with Ni 3d and 3s orbitals. Contributions from Ni 3d orbitals are designated with gray lines, whereas contributions from Ni 3s orbitals are depicted with black lines. The *y* axis of each plot corresponds to the COHP energy in eV. Negative deflections in the curves indicate bonding interactions; positive deflections are antibonding.

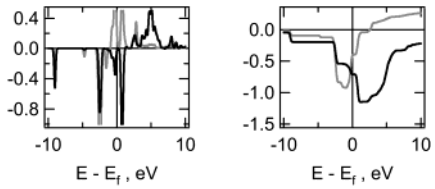

Figure 3. COHP curves (left plot) and integrals (right plot) for the overlap of C valence orbitals with Pd^2 4d and 4s orbitals in the μ-bridge configuration. Contributions from 4d orbitals are designated with gray lines, whereas contributions from 4s orbitals are depicted with black lines. The *y* axis of each plot corresponds to the COHP energy in eV. Negative deflections in the curves indicate bonding interactions; positive deflections are antibonding.

on the Ni(111) surface as compared to the Pd and Pt surfaces.[22] For the latter two metals, d orbitals play a more significant role in adsorbate binding,[58] potentially resulting in a shift in binding site preferences. Because the overlap of metal s orbitals with C−C antibonding orbitals is a major contribution to the COHP curve in the μ-bridge configuration, this configuration is expected to be more highly stabilized on Ni(111) than on other surfaces. For the purposes of comparison, we have also computed COHP curves for acetylene adsorption structures on Pd(111). Figure 3 shows the COHP curves and integrations for the overlap of Pd^2 atomic orbitals with antibonding orbitals of acetylene bound in the μ-bridge configuration. Although a significant overlap of the Pd^2 4s orbitals with C−C antibonding orbitals is still present at an energy 9 eV below the Fermi level, its integrated contribution to the bonding is much smaller (by ca. 0.3 eV) than in the case of Ni. Moving further down the periodic table, one would predict even less participation of the 5s orbitals in acetylene binding to Pt, perhaps offering an explanation for the instability of the μ-bridge structure on Pt-

(111). Moreover, because metal s orbital back-bonding is relatively smaller for the parallel-bridge configuration (see the top four plots in Figure 2), the stabilization of the latter structure on Ni would be expected to be less pronounced, consistent with the computed results in Table 3. Finally, the prevalence of back-bonding on Ni surfaces provides a satisfying explanation for the unique acetylene reactivity on Ni(111). The high degree of filling of C−C antibonding states for the Ni μ-bridge structure suggests that C−C bond scission should be particularly facile on Ni, consistent with the experimental results described above.

3.3. Implications for Acetylene Hydrogenation on Supported Catalysts. Numerous attempts have been made to understand the mechanism of acetylene hydrogenation over supported metal catalysts, with little consensus on the nature of the key surface processes and intermediates.[59,60] The calculated results presented above are clearly insufficient to clarify which of the proposed mechanisms is the "correct" one. However, our calculated results are consistent with the hypothesis that adsorbed acetylene and its decomposition products dominate the metal surface during acetylene hydrogenation. Because of its high binding energy above 3-fold hollow sites, acetylene would be expected to be highly effective in blocking high-coordination surface sites that may be required for interaction with ethylene. [49] The very strong adsorption of acetylene on the surface, which causes adsorbed C_2H_2 to be susceptible to decomposition, is also probably important in facilitating the formation of a carbonaceous layer.[59] Understanding the mechanism by which this carbonaceous layer can affect the adsorption and reaction of acetylene and ethylene requires further computational study of the energetics of acetylene reaction pathways. Further study of the mechanism by which hydrogen adsorption may affect the adsorption of acetylene[61] and accumulation of the carbonaceous material[6] is also warranted. Nevertheless, it seems reasonable to speculate that the adsorbed acetylene species reactive toward selective hydrogenation are in fact not the highly coordinated bridging species, which are bound very strongly to the metal surface.[4] Instead, the high-coordination sites may become irreversibly blocked by strongly adsorbed acetylene and its decomposition products, exposing only low-coordination sites for reversible adsorption and reaction.

It should be noted that our calculations cannot be used to identify factors controlling reaction selectivity and give no indication as to why acetylene hydrogenation should be more selective on the Pd surface. Differences in the reactions of acetylene on the surface following adsorption, including details of the production of a carbonaceous layer, may be responsible for the anomalous high selectivity for Pd catalysts. Further experimental and computational studies are therefore necessary to determine the causes for different acetylene hydrogenation performance among catalysts.

4. Conclusions

The adsorption of hydrogen and acetylene on the (111) surface plane of Pd, Pt, Ni, and Rh has been investigated using plane-wave DFT calculations. In agreement with previous experimental and computational studies, hydrogen is found to interact most favorably with 3-fold hollow sites on the surface, although the potential-energy surface is relatively flat for all metals, especially Pt. The most stable acetylene adsorption geometry was determined to be a 3-fold "parallel-bridge" configuration above the Pd, Pt, and Rh surfaces and a "μ-bridge" structure above the Ni surface. The anomalous adsorption properties of Ni are attributed to the high degree of overlap of Ni 3s orbitals with acetylene antibonding orbitals in the μ-bridge configuration. Generally, however, adsorption trends on the metals are similar, with computed binding energies in the range of 50−70 kcal/mol. The largely similar adsorption behavior of acetylene and hydrogen on these surfaces may help explain why all four metals are effective acetylene hydrogenation catalysts; however, differences observed among the different metal catalysts are most likely attributable to subsequent surface reactions of acetylene.

Acknowledgment. We gratefully acknowledge research support from the Electric Power Research Institute (EPRI). Sandia is a multiprogram laboratory operated by Sandia Corporation, a Lockheed Martin Company, for the United States Department of Energy under Contract DE-AC04-94-AL85000.

References and Notes

(1) Bos, A. N. R.; Bootsma, E. S.; Foeth, F.; Sleyster, H. W. J.; Westerterp, K. R. *Chem. Eng. Process.* **1993**, *32*, 53.
(2) Bond, G. C.; Wells, P. B. *Adv. Catal.* **1964**, *15*, 91.
(3) Thomson, S. J.; Webb, G. *J. Chem. Soc. Chem. Commun.* **1976**, 526.
(4) Houzvicka, J.; Pestman, R.; Ponec, V. *Catal. Lett.* **1995**, *30*, 289.
(5) Al-Ammar, A. S.; Webb, G. *J. Chem. Soc., Faraday Trans. 1* **1978**, *1*, 195.
(6) Al-Ammar, A. S.; Webb, G. *J. Chem. Soc., Faraday Trans. 1* **1978**, *74*, 657.
(7) Al-Ammar, A. S.; Webb, G. *J. Chem. Soc., Faraday Trans. 1* **1979**, *75*, 1900.
(8) Davis, S. M.; Zaera, F.; Somorjai, G. A. *J. Catal.* **1982**, *77*, 439.
(9) Bos, A. N. R.; Westerterp, K. R. *Chem. Eng. Process.* **1993**, *32*, 1.
(10) Janssens, T. V. W.; Volkening, S.; Zambelli, T.; Wintterlin, J. *J. Phys. Chem. B* **1998**, *102*, 6521.
(11) Cremer, P. S.; Su, X.; Shen, Y. R.; Somorjai, G. A. *J. Phys. Chem. B* **1997**, *101*, 6474.
(12) Zhu, X.-Y.; White, J. M. *Surf. Sci.* **1989**, *214*, 240.
(13) Mate, C. M.; Kao, C.-T.; Bent, B. E.; Somorjai, G. A. *Surf. Sci.* **1988**, *197*, 183.
(14) Ormerod, R. M.; Lambert, R. M.; Bennett, D. W.; Tysoe, W. T. *Surf. Sci.* **1995**, *330*, 1.
(15) Sandell, A.; Beutler, A.; Jaworski, A.; Wiklund, M.; Heister, K.; Nyholm, R.; Andersen, J. N. *Surf. Sci.* **1998**, *415*, 411.
(16) Stacchiola, D.; Molero, H.; Tysoe, W. T. *Catal. Today* **2001**, *65*, 3.
(17) van Santen, R. A.; Neurock, M. *Catal. Rev.-Sci. Eng.* **1995**, *37*, 557.
(18) Watwe, R. M.; Spiewak, B. E.; Cortright, R. D.; Dumesic, J. A. *J. Catal.* **1998**, *180*, 184.
(19) Clotet, A.; Pacchioni, G. *Surf. Sci.* **1996**, *346*, 91.
(20) Fahmi, A.; van Santen, R. A. *Surf. Sci.* **1997**, *371*, 53.
(21) Dong, W.; Ledentu, V.; Sautet, P.; Eichler, A.; Hafner, J. *Surf. Sci.* **1998**, *411*, 123.
(22) Papoian, G. A.; Norskov, J. K.; Hoffmann, R. *J. Am. Chem. Soc.* **2000**, *122*, 4129.
(23) Michaelides, A.; Hu, P. *J. Chem. Phys.* **2000**, *112*, 6006.
(24) Payne, M. C.; Teter, M. P.; Allan, D. C.; Arias, T. A.; Joannopoulos, J. D. *Rev. Mod. Phys.* **1992**, *64*, 1045.
(25) Perdew, J. P.; Chevary, J. A.; Vosko, S. H.; Jackson, K. A.; Pederson, M. R.; Singh, D. J.; Fiolhais, C. *Phys. Rev. B* **1992**, *46*, 6671.
(26) Laasonen, K.; Pasquarello, A.; Car, R.; Lee, C.; Vanderbilt, D. *Phys. Rev. B* **1993**, *46*, 6671.
(27) Monkhorst, H. J.; Pack, J. D. *Phys. Rev. B* **1976**, *13*, 5188.
(28) Landrum, G. A.; Glassey, W. V. 2001; http://yaehmop.sourceforge.net.
(29) Hoffmann, R. *J. Chem. Phys.* **1963**, *39*, 1397.
(30) Hoffmann, R. *J. Chem. Phys.* **1964**, *40*, 2474.
(31) Hoffmann, R. *J. Chem. Phys.* **1964**, *40*, 2745.
(32) Dronskowski, R.; Blochl, P. E. *J. Chem. Phys.* **1993**, *97*, 8613.
(33) Glassey, W. V.; Papoian, G. A.; Hoffmann, R. *J. Chem. Phys.* **1999**, *111*, 893.
(34) Behm, R. J.; Penka, V.; Cattania, M. G.; Christmann, K. R.; Ertl, G. *J. Chem. Phys.* **1983**, *78*, 7486.
(35) Yanagita, H.; Fujioka, H.; Aruga, T.; Takagi, N.; Nishijima, M. *Surf. Sci.* **1999**, *441*, 507.
(36) Yang, H.; Whitten, J. L. *J. Chem. Phys.* **1993**, *98*, 5039.
(37) Watson, G. W.; Wells, R. P. K.; Willock, D. J.; Hutchings, G. J. *J. Phys. Chem. B* **2001**, *105*, 4889.
(38) Cattania, M. G.; Christmann, K. R.; Penka, V.; Ertl, G. *Gazz. Chim. Ital.* **1983**, *113*, 433.
(39) Nieuwenhuys, B. E. *Surf. Sci.* **1976**, *65*, 369.

(40) Godbey, D. J.; Somorjai, G. A. *Surf. Sci.* **1988**, *204*, 301.
(41) Atli, A.; Alnot, M.; Ehrhardt, J. J.; Bertolini, J. C.; Abon, M. *Surf. Sci.* **1992**, *269/270*, 365.
(42) Christmann, K.; Schober, O.; Ertl, G.; Neumann, M. *J. Chem. Phys.* **1974**, *60*, 4528.
(43) Yates, J. T.; Thiel, P. A.; Weinberg, W. H. *Surf. Sci.* **1979**, *84*, 427.
(44) Gorodetskii, V. V.; Nieuwenhuys, B. E.; Sachtler, W. M. H.; Boreskov, G. K. *Surf. Sci.* **1981**, *108*, 225.
(45) Hoffman, H.; Zaera, F.; Ormerod, R. M.; Lambert, R. M.; Yao, J. M.; Saldin, D. K.; Wang, L. P.; Bennett, D. W.; Tysoe, W. T. *Surf. Sci.* **1992**, *268*, 1.
(46) Tysoe, W. T.; Nyberg, G. L.; Lambert, R. M. *Surf. Sci.* **1983**, *135*, 128.
(47) Vattuone, L.; Yeo, Y. Y.; Kose, R.; King, D. A. *Surf. Sci.* **2000**, *447*, 1.
(48) Stacchiola, D.; Burkholder, I.; Tysoe, W. T. *Surf. Sci.* **2002**, *511*, 215.
(49) Neurock, M.; Pallassana, V.; van Santen, R. A. *J. Am. Chem. Soc.* **2000**, *122*, 1150.
(50) Spiewak, B. E.; Cortright, R. D.; Dumesic, J. A. *J. Catal.* **1998**, *176*, 405.
(51) Kose, R.; Brown, W. A.; King, D. A. *J. Am. Chem. Soc.* **1999**, *121*, 4845.
(52) Megiris, C. E.; Berlowitz, P.; Butt, J. B.; Kung, H. H. *Surf. Sci.* **1985**, *159*, 184.
(53) Dubois, L. H.; Castner, D. G.; Somorjai, G. A. *J. Chem. Phys.* **1980**, *72*, 5234.
(54) Papageorgopoulos, D. C.; Ge, Q.; Nimmo, S.; King, D. A. *J. Phys. Chem. B* **1997**, *101*, 1999.
(55) Parker, W. L.; Siedle, A. R.; Hexter, R. M. *J. Am. Chem. Soc.* **1985**, *107*, 264.
(56) Bao, S.; Hofmann, P.; Schindler, K.-M.; Fritzsche, V.; Bradshaw, A. M.; Woodruff, D. P.; Casado, C.; Asensio, M. C. *J. Phys. Condens. Matter* **1994**, *6*, L93.
(57) Bond, G. C. *Catalysis by Metals*; Academic Press: New York, 1962.
(58) Demuth, J. E. *Surf. Sci.* **1977**, *65*, 369.
(59) Borodzinski, A.; Golebiowski, A. *Langmuir* **1997**, *13*, 883.
(60) Vincent, M. J.; Gonzalez, R. D. *Appl. Catal. A* **2001**, *217*, 143.
(61) Molero, H.; Bartlett, B. F.; Tysoe, W. T. *J. Catal.* **1999**, *181*, 49.